Electromagnetic dissociation of nuclei in heavy-ion collisions

C. J. Benesh
Theoretical Division, Los Alamos National Laboratory, Los Alamos, New Mexico 87545

J. L. Friar
Theoretical Division, Los Alamos National Laboratory, Los Alamos, New Mexico 87545
and Institut für Kernphysik, Johannes Gutenberg-Universität, D-6500 Mainz, Germany
(Received 28 December 1992)

Large discrepancies have been observed between measured electromagnetic dissociation (ED) cross sections and the predictions of the semiclassical Weizäcker-Williams-Fermi (WWF) method. In this paper, the validity of the semiclassical approximation is examined. The total cross section for electromagnetic excitation of a nuclear target by a spinless projectile is calculated in first Born approximation, neglecting recoil. The final result is expressed in terms of correlation functions and convoluted densities in configuration space. The result agrees with the WWF approximation to leading order (unretarded electric dipole approximation), but the method allows an analytic evaluation of the cutoff, which is determined by the details of the electric dipole transition charge density. Using the Goldhaber-Teller model of that density, and uniform charge densities for both projectile and target, the cutoff is determined for the total cross section in the nonrelativistic limit, and found to be smaller than values currently used for ED calculations. In addition, cross sections are calculated using a phenomenological momentum space cutoff designed to model final state interactions. For moderate projectile energies, the calculated ED cross section is found to be smaller than the semiclassical result, in qualitative agreement with experiment.

PACS number(s): 25.75.+r

I. INTRODUCTION

The availability of relativistic heavy-ion beams has opened a new avenue for the study of electromagnetic excitations of nuclei. Cross sections are enhanced both by the charge of the projectile ions and by the relativistic contraction of the projectile's electric field into a sharp pulse of radiation at high energies. Experiments range from single and double nucleon-removal reactions [1], to the study of "halo" nuclei using radioactive beams [2], to the possibility of multiphonon excitations of collective nuclear states [3]. Aside from their intrinsic interest, electromagnetic excitation processes in peripheral collisions will also be important at the Brookhaven Relativistic Heavy Ion Collider (RHIC) [4].

There is, therefore, a tremendous incentive to develop an understanding of the physics involved in these processes. Such an understanding has two facets. On the one hand, one must be able to calculate the detailed structure of the target nucleus in order to calculate its response to a particular probe, such as the electromagnetic interaction. Fortunately, this has been one of the central topics of nuclear physics for many years, and an extensive literature exists on the subject [5]. On the other hand, it is also necessary to understand the process by which the projectile excites the target. With few exceptions to date [6], this aspect of the problem has been dealt with by using the venerable Weizäcker-Williams-Fermi (WWF) method of virtual quanta [7], and its generalization to arbitrary multipoles [8]. This approach is based on the observation, due to Fermi, that the electromagnetic fields of a point charge, when boosted to high energy, are transverse to the direction of the charge's motion. The supposition is that one can calculate cross sections by replacing the projectile by an equivalent pulse of electromagnetic radiation. The cross section for a given reaction is then

$$\sigma_{\rm WW} = \int d\omega\, n(\omega)\, \sigma_\gamma(\omega), \tag{1}$$

where $\sigma_\gamma(\omega)$ is the cross section for the same reaction induced by real photons, and $n(\omega)$ is the number of photons of energy ω in the pulse of equivalent radiation. For dipole transitions, $n(\omega)$ can be determined by calculating the intensity of the projectile fields as a function of frequency, integrated over impact parameters [9]. Assuming the projectile's trajectory is a straight line, the result is

$$n_{E1}(\omega) = \frac{2Z_p^2\alpha}{\pi\beta^2\omega}\left(xK_0(x)K_1(x) - \frac{\beta^2}{2}x^2[K_1^2(x) - K_0^2(x)]\right) \sim \frac{2Z_p^2\alpha}{\pi\beta^2\omega}\left[\ln\left(\frac{1.123}{x}\right) - \frac{\beta^2}{2}\right] \quad \text{as } \gamma \to \infty\,, \tag{2}$$

where $K_{0(1)}$ is a Bessel function of imaginary argument, Z_p is the projectile charge, β its speed, $x = \frac{\omega b_{\rm min}}{\gamma\beta}$, and $b_{\rm min}$ is an impact parameter cutoff required to get a finite result.

In some respects, the Weizäcker-Williams-Fermi (WWF) method is very well suited to the problem of electromagnetic dissociation by heavy ions. Cross sections may be calculated either using a model or, as is often

done, by direct appeal to measured photodisintegration cross sections. In the latter case one obtains a cross section, at least at high energy [10], that is independent of any model of the target's structure. Furthermore, the equivalent photon number, $n(\omega)$, can be obtained by a relatively straightforward classical calculation. Nonetheless, the WWF method is not completely satisfactory. Theoretically, there is no systematic procedure for evaluating corrections to the semiclassical result, and consequently no way of gauging the reliability of the approach. In addition, there is the troublesome problem of choosing the minimum impact parameter. Since $b_{\min}$ is not fixed by the WWF procedure itself, a number of choices have been proposed [11], based on phenomenological considerations. On the experimental side, large discrepancies from the naive WWF predictions have been observed in target fragmentation experiments [12], leading some authors to question the validity of first-order perturbation theory for heavy projectiles [13].

The aim of this paper is to go beyond the semiclassical WWF method and calculate the quantum mechanical cross section for electromagnetic excitation of nuclei in heavy-ion collisions. In the next section we derive an expression, originally used in high energy physics [14], for the unpolarized cross section in first Born approximation, neglecting recoil effects for both the projectile and target nuclei. We demonstrate that the cross section does approach the WWF approximation in the limit of large projectile energy, and in an Appendix we derive an expression for the cutoff parameter, $b_{\min}$, for dipole transitions, using a simple model for the transition matrix elements. In the following section we use the same simple model to compare our results for the full cross section to those of the WWF approximation as a function of projectile energy, transition multipolarity, and transition frequency. Finally, using a phenomenological cutoff designed to model final-state interaction effects, we compare the results of this simple model with measured single-neutron removal cross sections.

II. QUANTUM EXCITATION CROSS SECTION

We begin this section with a discussion of the kinematics of the nuclear excitation process. The projectile nucleus, with mass M_1 and momentum $P_i^\mu = (E_i, \mathbf{P}_i)$, scatters from the target by exchanging a virtual photon of momentum q^μ. In the process, depicted in Fig. 1, the target of mass M_2 is excited from its ground state to an excited state of mass $M_2 + \omega$. For high Z_p projectiles, elastic scattering of the projectile ($\propto Z_p^2$) will dominate over inelastic processes ($\propto Z_p$), so that in the following we shall assume that the projectile remains unexcited in the final state. This is in accord with the semiclassical picture, where the projectile remains in its ground state, following a straight line trajectory throughout the collision. Kinematically, the elastic scattering of the projectile translates into a condition on the four-momentum transfer q,

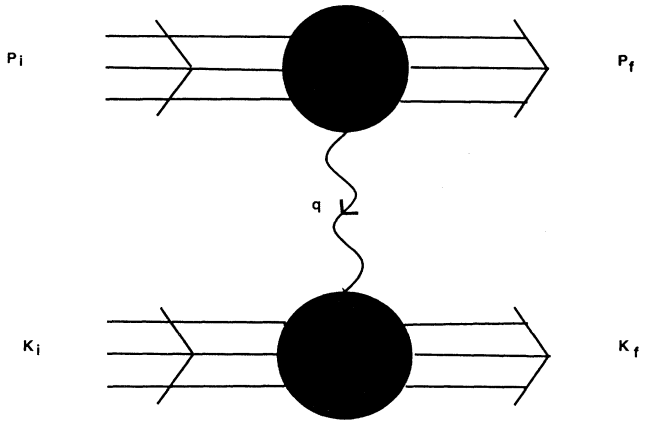

FIG. 1. Electromagnetic excitation process.

$$q^2 = 2P_i \cdot q \rightarrow q^2 = 2E_i(q_0 - \boldsymbol{\beta} \cdot \mathbf{q}), \tag{3}$$

where $\boldsymbol{\beta} = \mathbf{P}_i/E_i$ is the projectile velocity. For nuclear transitions, the momentum and energy transfers are on the order of tens of MeV, while the projectile and target masses are on the order of tens of GeV. As a result, $q^2/2E_i$ is negligible, and we immediately obtain the minimum momentum transfer

$$|\,\mathbf{q}\,|_{\min} = q_0/\beta \rightarrow q^2_{\min} = -\frac{q_0^2}{\gamma^2\beta^2}, \tag{4}$$

where $\gamma = \frac{1}{\sqrt{1-\beta^2}}$. In exactly the same fashion, we derive a relation between the energy transfer and the target excitation energy,

$$q_0 = \omega + \mathcal{O}(\omega^2/M_2). \tag{5}$$

Even at this stage of the calculation, we see a similarity with the semiclassical calculation at high energy. For large projectile energies, the minimum momentum transfer goes to zero, so that it is reasonable to expect that the cross section will be dominated by the pole in the photon propagator at $q^2 = 0$, where the interaction cross section will be well approximated by the cross section for real photons.

Having treated the kinematics, we now turn to the calculation of the cross section. The method we use is a straightforward evaluation of the Feynman diagram of Fig. 1, borrowing heavily from the theory of relativistic electron scattering [15] in order to relate the target and projectile form factors to the appropriate nuclear transition matrix elements. For a 0^+ projectile (the generalization to nonzero spin is trivial), the spin-averaged cross section for an arbitrary transition multipole is given by

$$\sigma_{\rm WW} = -\frac{(4\pi Z_p\alpha)^2}{[(P_i\cdot K_i)^2 - M_1^2M_2^2]^{1/2}} \int \frac{d^4q}{(2\pi)^4}\frac{d^3P_f}{2E_f(2\pi)^3}(2\pi)^4\delta^4(P_f - P_i + q)F_p^2(q^2)P_i^\mu P_i^\nu W^T_{\mu\nu}(q^2, q\cdot K_i), \tag{6}$$

where the matrix element of the projectile current is given by $Z_p F_p(q^2)\,(P_{i\mu} + \frac{q_\mu}{2})$, and the spin-averaged target structure function is given by

$$W^T_{\mu\nu}(q^2, q\cdot K_i) = \int \frac{d^3K_f}{(2E_{K_f})(2\pi)^3}(2\pi^4)\delta^4(K_f - K_i - q)\frac{1}{(2J_i+1)}\sum_{mm'}\langle K_i, m|J_\mu(0)|K_f, m'\rangle\langle K_f, m'|J_\nu(0)|K_i, m\rangle \quad (7)$$

$$= W_1(q^2, q\cdot K_i)\left(g_{\mu\nu} - \frac{q_\mu q_\nu}{q^2}\right) + W_2(q^2, q\cdot K_i)\left(K_{i\mu} - \frac{q\cdot K_i q_\mu}{q^2}\right)\left(K_{i\nu} - \frac{q\cdot K_i q_\nu}{q^2}\right), \quad (8)$$

where m (m') denote the azimuthal angular momentum quantum numbers of the initial (final) state, $(E_{K_f}, \mathbf{K}_f)$ is the final state four-momentum, and $W_1(q^2, q\cdot K_i)$ and $W_2(q^2, q\cdot K_i)$ are Lorentz invariant target structure functions. For what follows, it is critical to realize that while the structure functions $W_1(q^2, q\cdot K_i)$ and $W_2(q^2, q\cdot K_i)$ are different for different transition multipoles, the tensor form of $W^T_{\mu\nu}$ is determined by current conservation and parity, and thus independent of both the multipolarity of the transition and spin of the target. Using the elastic scattering condition for the projectile, and keeping only the leading terms in inverse powers of the projectile and target masses, we get

$$\sigma_{\rm WW} = -\frac{(4\pi Z_p\alpha)^2}{[(P_i\cdot K_i)^2 - M_1^2M_2^2]^{1/2}}\int \frac{d^4q}{(2\pi)^4}\frac{d^3P_f}{2E_f(2\pi)^3}(2\pi)^4\delta^4(P_f - P_i + q)\,F_p^2(q^2)$$
$$\times\Big[M_1^2W_1(q^2, q\cdot K_i) + (P_i\cdot K_i)^2W_2(q^2, q\cdot K_i)\Big]. \quad (9)$$

At this point, it is useful to reexpress the two invariant structure functions in terms of nuclear matrix elements. In particular, we shall choose the two rotationally invariant combinations $\langle J_0(0)J_0(0)\rangle \equiv \langle\rho(0)\rho(0)\rangle$ and $\langle\mathbf{J}(0)\cdot\mathbf{J}(0)\rangle$, where the brackets are introduced as a convenient shorthand for the spin sums and matrix elements of Eq. (7). Hence, in the target rest frame,

$$W_1(q^2, q\cdot K_i) = \int \frac{d^3K_f}{(2E_{K_f})(2\pi)^3}(2\pi)^4\delta^4(K_f - K_i - q)\frac{-\mathbf{q}^2\langle\mathbf{J}(0)\mathbf{J}(0)\rangle + q_0^2\langle\rho(0)\rho(0)\rangle}{2\mathbf{q}^2}, \quad (10)$$

$$W_2(q^2, q\cdot K_i) = \int \frac{d^3K_f}{(2E_{K_f})(2\pi)^3}(2\pi)^4\delta^4(K_f - K_i - q)\frac{q^2}{M_2^2}\frac{(2q^2 + q_0^2)\langle\rho(0)\rho(0)\rangle - \mathbf{q}^2\langle\mathbf{J}(0)\cdot\mathbf{J}(0)\rangle}{\mathbf{q}^4}. \quad (11)$$

For analytical purposes, it is convenient to have expressions in configuration space. Replacing the momentum δ functions by an integral representation, and using translational invariance, we obtain

$$W_1(q^2, q\cdot K_i) = \int \frac{d^3K_f}{(2E_{K_f})(2\pi)^3}(2\pi)\delta(E_{K_f} - M_2 - q^0)\int d^3z\, e^{i\mathbf{q}\cdot\mathbf{z}}\frac{-\mathbf{q}^2\langle\mathbf{J}(\mathbf{z})\cdot\mathbf{J}(0)\rangle + q_0^2\langle\rho(\mathbf{z})\rho(0)\rangle}{2\mathbf{q}^2}, \quad (12)$$

$$W_2(q^2, q\cdot K_i) = \int \frac{d^3K_f}{(2E_{K_f})(2\pi)^3}(2\pi)\delta(E_{K_f} - M_2 - q^0)\frac{q^2}{M_2^2}\int d^3z\, e^{i\mathbf{q}\cdot\mathbf{z}}\frac{(2q^2 + q_0^2)\langle\rho(\mathbf{z})\rho(0)\rangle - \mathbf{q}^2\langle\mathbf{J}(\mathbf{z})\cdot\mathbf{J}(0)\rangle}{\mathbf{q}^4}. \quad (13)$$

The projectile form factor is related to the projectile *rest frame* charge density via

$$F(q^2) = \int d^3x e^{i\mathbf{q}'\cdot\mathbf{x}}\rho_p(\mathbf{x}), \quad (14)$$

where $\mathbf{q}' = \mathbf{q} - \frac{(\gamma-1)}{\gamma\beta^2}\boldsymbol{\beta}\cdot\mathbf{q}\boldsymbol{\beta}$ is the three-momentum transfer in the projectile rest frame.

Since the matrix elements appearing here are rotational scalars, we may replace the complex exponential by its angular average with impunity. The result for the cross section then becomes, after performing the integrations over the three-momentum transfer,

$$\sigma_{\rm WW} = \frac{2(Z_p\alpha)^2}{\beta^2}\int\frac{dq^0}{(q^0)^2}\int\frac{d^3K_f}{(2\pi)^32E_{K_f}}(2\pi)\delta(E_{K_f} - M_2 - q^0)$$
$$\times\int d^3z\Big[\langle\rho_c(\mathbf{z})\rho_c(0) - \mathbf{J}_c(\mathbf{z})\cdot\mathbf{J}_c(0)\rangle\left(\frac{1}{\gamma^2}I_1(q_0z,\beta) + I_2(q_0z,\beta)\right)$$
$$+\langle\rho_c(\mathbf{z})\rho_c(0)\rangle\left(\frac{1}{\gamma^2}I_2(q_0z,\beta) + I_3(q_0z,\beta)\right)\Big], \quad (15)$$

where

$$I_1(y,\beta) = \int_{\frac{1}{\beta}}^{\infty} q\,dq\frac{j_0(qy)}{(1-q^2)^2}$$
$$= \frac{1}{4y}\{[\mathrm{Si}((1/\beta - 1)y) - \mathrm{Si}((1/\beta + 1)y)](\cos y + y\sin y)$$
$$+[\mathrm{Ci}((1/\beta + 1)y) + \mathrm{Ci}((1/\beta - 1)y)](\sin y - y\cos y) + 2\beta\gamma^2\sin(y/\beta)\}, \quad (16)$$

$$I_2(y,\beta) = \int_{\frac{1}{\beta}}^{\infty} q\,dq \frac{j_0(qy)}{q^2(1-q^2)}$$
$$= \frac{1}{y}\{\tfrac{1}{2}\cos y[\mathrm{Si}((1/\beta-1)y) - \mathrm{Si}((1/\beta+1)y)]$$
$$+\tfrac{1}{2}\sin y[\mathrm{Ci}((1/\beta+1)y) + \mathrm{Ci}((1/\beta-1)y)] + \beta\sin(y/\beta) - y\mathrm{Ci}(y/\beta)\}, \quad (17)$$

$$I_3(y,\beta) = 3\int_{\frac{1}{\beta}}^{\infty} \frac{q\,dq}{q^4} j_0(qy)$$
$$= (\beta^2 - y^2/2)j_0(y/\beta) + \frac{\beta^2}{2}\cos(y/\beta) + \frac{y^2}{2}\mathrm{Ci}(y/\beta), \quad (18)$$

with $\mathrm{Si}(y)$ and $\mathrm{Ci}(y)$ the sine and cosine integral functions, respectively, and

$$\rho_c(\mathbf{z}) = \frac{\gamma}{Z_p}\int d^3x\rho_p\left(\mathbf{x} + \frac{(\gamma-1)}{\beta^2}\boldsymbol{\beta}\boldsymbol{\beta}\cdot\mathbf{x}\right)\rho(\mathbf{z}-\mathbf{x}), \quad (19)$$

$$\mathbf{J}_c(\mathbf{z}) = \frac{\gamma}{Z_p}\int d^3x\mathbf{J}_p\left(\mathbf{x} + \frac{(\gamma-1)}{\beta^2}\boldsymbol{\beta}\boldsymbol{\beta}\cdot\mathbf{x}\right)\rho(\mathbf{z}-\mathbf{x}).$$

At this juncture, the expression bears little resemblance to the compact semi-classical result in Eqs. (1) and (2). There is no simple factorization of the integrand into a flux factor multiplying the photonuclear cross section. The integrand is not even a function of the same variable, $q^0/\gamma\beta$, as the expressions in Eq. (1). Asymptotically, the cross section of Eq. (14) falls off like a power for large q^0, in contrast to the exponential decrease dictated by the Bessel functions of the semiclassical result. In light of this, it seems quite unlikely that the semiclassical expression will yield a good approximation for the cross section over a large energy range.

On the other hand, the correspondence principle tells us that the two expressions must agree in the classical limit. For the problem at hand, the classical regime occurs for large projectile energies, where the straight line trajectory of the projectile represents a good approximation to the classical trajectory. In that limit ($\gamma \to \infty$), the momentum integrals become

$$I_1(y,\beta) \approx \frac{\gamma^2}{2}j_0(y) + \mathcal{O}(1), \quad (20)$$
$$I_2(y,\beta) \approx -j_0(y)\ln(\gamma) + \mathcal{O}(1), \quad (21)$$
$$I_3(y,\beta) \approx \mathcal{O}(1), \quad (22)$$

and the cross section is given by

$$\sigma_{\mathrm{WW}} = \frac{(Z_p\alpha)^2}{\beta^2}\int\frac{dq^0}{(q^0)^2}\int\frac{d^3K_f}{(2\pi)^3 2E_{K_f}}(2\pi)\delta(E_{K_f} - M_2 - q^0)$$
$$\times\int d^3z[\langle\rho_c(\mathbf{z})\rho_c(0) - \mathbf{J}_c(\mathbf{z})\cdot\mathbf{J}_c(0)\rangle\, j_0(q^0z)\,(1-\ln(\gamma^2)) + \mathcal{O}(1)]. \quad (23)$$

Using methods identical to those just described, the cross section for real photons can be written as

$$\sigma_\gamma(q^0) = -\frac{\pi\alpha}{q^0}\int\frac{d^3K_f}{(2\pi)^3 2E_{K_f}}(2\pi)\delta(E_{K_f} - M_2 - q^0)$$
$$\times\int d^3z\, j_0(q^0z)\langle\rho(\mathbf{z})\rho(0) - J(\mathbf{z})J(0)\rangle. \quad (24)$$

From which it follows that (γ_E is Euler's constant)

$$\sigma_{\mathrm{WW}} = \frac{2(Z_p\alpha)^2}{\beta^2}\int\frac{dq^0}{(q^0)^2}\left\{\left[\ln\left(\frac{2\gamma}{q^0R_\ell}\right) - \gamma_E - \frac{1}{2}\right]\right.$$
$$\left.\times\frac{q^0\sigma_\gamma(q^0)}{\pi\alpha} + \mathcal{O}(1/\gamma^2)\right\}, \quad (25)$$

where all the terms of order $(1/\gamma)^0$ have been absorbed into the cutoff parameter R_ℓ.

The first term in this expression is just the high energy limit of the semiclassical cross section, with no cutoff parameter. The cutoff parameter, R_ℓ, represents the leading order corrections due to Coulomb and longitudinally polarized virtual photons, as well as off-shell corrections to the photonuclear cross section. In the limit of large γ, the precise value of $\ln(q^0R_\ell)$ will be negligible compared to $\ln(\gamma)$, and the semiclassical result is recovered.

In the low frequency limit, the off-shell corrections to the photonuclear cross section vanish, and R_ℓ is determined solely by the projectile and target transition densities. In Appendix B we exploit this fact to calculate R_1, using the Goldhaber-Teller model [16] for the transition densities. Accurate determination of this parameter, which governs the *total* excitation cross section, will be relevant for estimating the large background due to electromagnetic processes at RHIC, where the semiclassical limit should be realized.

Once R_1 is determined, the cross section can be expressed in a particularly simple and elegant form which

emphasizes well-known photonuclear sum rules. In Appendix B we find

$$\sigma_{\rm WW} = \frac{2\alpha\,\sigma_{-1}Z_p^2}{\pi\beta^2}\left[\ln\left(\frac{2\beta\gamma}{\bar{\omega}R_1}\right) - \gamma_E - \frac{\beta^2}{2}\right], \quad \text{(B23)}$$

where σ_{-1} is defined in Eq. (A9) and has the experimental value, $0.22(2)A_t^{\frac{4}{3}}$ mb for medium to heavy nuclei, and $\bar{\omega}$ is the mean photon energy, which can be taken to be the giant resonance energy, $79A_t^{-\frac{1}{3}}$ MeV see [21]. The factors in front of the bracket are (numerically) consistent with $Z_p^2A_t^{\frac{4}{3}}/\beta^2\,\mu$b. The argument of the logarithm is $\xi\beta\gamma$, where ξ varies from 6.0 to 4.3 as R_p varies from 0 to R_t.

III. RESULTS

In this section we compare results both with the semiclassical calculations using the Weizäcker-Williams method and, ultimately, with data from single neutron removal experiments. To do this, we are required to assume a model for the transition matrix elements appearing in Eq. (14). Since the emphasis here is on a comparison of the quantum and semiclassical methods rather than a detailed description of data, we shall postpone many of the nuclear structure details (realistic transition densities, widths, fractional saturation of the energy weighted sum rules, etc.) for later consideration. For simplicity's sake, we again choose the Goldhaber-Teller (GT) [16] model to describe the transition densities, and assume that the projectile and target are described by uniform density spheres. A brief sketch of the GT model, as applied to dipole excitations, may be found in the Appendix. For general multipoles, a more detailed description of the model, including electromagnetic transition matrix elements, may be found in Ref. [15].

In order to effect a comparison with the semiclassical calculation for arbitrary γ, it is useful to decompose the total cross section into multipoles. Since the magnetic multipole contributions to the cross section are small, we shall restrict our attention to electric multipoles larger than zero. The decomposition may be accomplished by inserting a factor

$$1 = \frac{1}{V}\int d^3x\,d^3x'\delta^3(\mathbf{z}-\mathbf{x}+\mathbf{x}'), \quad (26)$$

into Eq. (14), and by using the Bessel function identity

$$j_0(q|\mathbf{x}-\mathbf{x}'|) = 4\pi\sum_{\ell m} j_\ell(qx)j_\ell(qx')Y_{\ell m}(\hat{x})Y^*_{\ell m}(\hat{x}'), \quad (27)$$

to do the angular integrals. The result is

$$\sigma_{\rm WW} = \frac{2(Z_p\alpha)^2}{\beta^2}\sum_\ell\int dq^0\delta(q^0-\omega_\ell)\int_{q_0/\beta}^\infty q\,dqF_p^2(q') \times\left[\frac{1}{\gamma^2}\frac{F_\rho^\ell(q)-F_J^\ell(q)}{(q_0^2-q^2)^2} + \frac{F_\rho^\ell(q)-F_J^\ell(q)}{(q_0^2-q^2)q^2} + \frac{F_\rho^\ell(q)}{q^4} + \frac{1}{\gamma^2}\frac{F_\rho^\ell(q)}{(q_0^2-q^2)q^2}\right], \quad (28)$$

where, for $\ell > 0$, $F_\rho^\ell(q) = \ell C_\ell j_\ell^2(qR_t)$, and $F_J^\ell(q) = \frac{(2\ell+1)}{\ell}\frac{q_0^2}{q^2}F_\rho^\ell(q)$, with R_t the radius of the target nucleus and C_ℓ a constant chosen such that the photonuclear cross section satisfies the energy weighted sum rule for multipole ℓ, and $F_p(q') = 3j_1(q'R_p)/q'R_p$ is the elastic form factor of the projectile, with R_p the projectile radius.

For comparison, we also calculate the semiclassical cross section in the same model, using a prescription from Ref. [11] for the minimum impact parameter,

$$b_{\rm min} = 1.34\left[A_p^{1/3} + A_t^{1/3} - 0.75(A_p^{-1/3} + A_t^{-1/3})\right], \quad (29)$$

appropriate for single and double nucleon removal experiments. The ratio of the quantum and semiclassical cross sections for ^{12}C and ^{197}Au projectiles incident on a ^{197}Au target are shown, as a function of projectile energy, in Figs. 2 and 3, respectively, for both $E1$ and $E2$ transitions. We assume that the $E1$ ($E2$) transition is to a

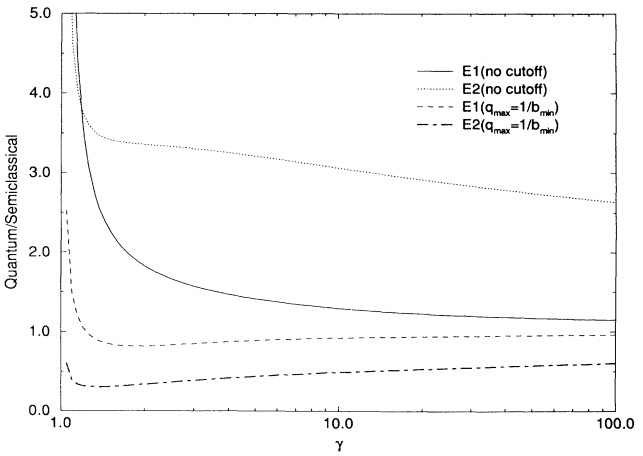

FIG. 2. Ratio of the quantum to classical excitation cross sections for ^{12}C on ^{197}Au as a function of projectile energy. The solid and dotted curves result from the full quantum mechanical calculation assuming no cutoff on the transverse momentum transfer, while the dashed and dot-dashed curves include a cutoff $q_{\rm max} = 1/b_{\rm min}$.

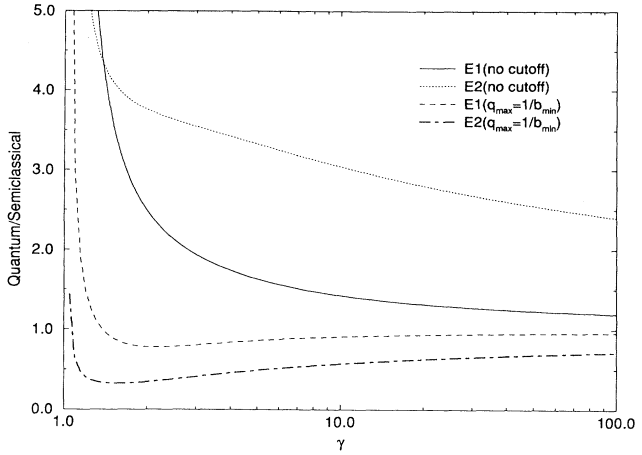

FIG. 3. Ratio of the quantum to semiclassical excitation cross sections for ^{197}Au on ^{197}Au as a function of projectile energy. The solid and dotted curves result from the full quantum mechanical calculation assuming no cutoff on the transverse momentum transfer, while the dashed and dot-dashed curves include a cutoff $q_{\max} = 1/b_{\min}$.

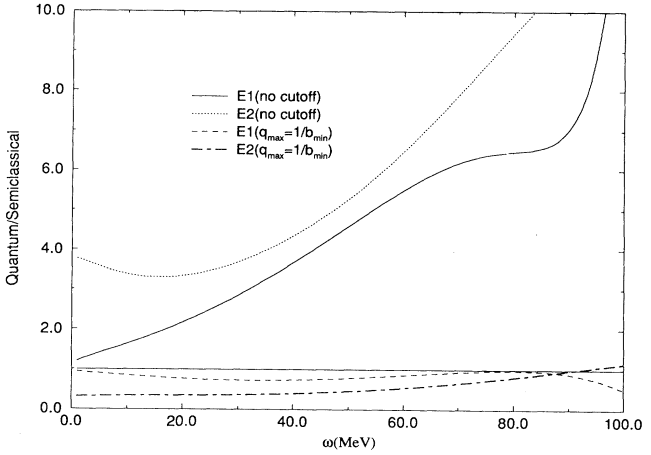

FIG. 4. Ratio of the quantum to classical excitation cross sections for ^{12}C on ^{197}Au as a function of transition energy. The solid and dotted curves result from the full quantum mechanical calculation assuming no cutoff on the transverse momentum transfer, while the dashed and dot-dashed curves include a cutoff $q_{\max} = 1/b_{\min}$.

sharp, isovector (isoscalar) giant resonance state at 13.8 (11.0) MeV, and that the energy weighted sum rule is saturated. We further assume that the giant resonance state decays exclusively via one neutron emission. For high projectile energies, we find that the quantum $E1$ cross section is enhanced by about 10% relative to the classical result. This enhancement agrees with the results of the Appendix, where it was shown that the quantum mechanical cutoff is smaller than that of Eq. [29], resulting in a larger cross section. More surprising is the enhancement of the $E2$ cross section, which remains a factor of 2 larger than the classical result at γ=100. Also noteworthy is the huge enhancement of both the quantum $E1$ and $E2$ cross sections at small projectile energies. For $\gamma > 5$, nearly all of the difference in the $E1$ cross section may be reabsorbed into a redefinition of $b_{\min}$ as described in the Appendix, so we conclude that the WWF method is a good approximation for the total $E1$ cross section for energies of 5 GeV/nucleon and higher, provided that the minimum impact parameter is properly chosen. For lower energies, much of the difference can be eliminated by altering $b_{\min}$, but discrepancies as large as 20% persist at very low projectile energies.

In Figs. 4 and 5, the ratio of the quantum and semiclassical cross sections is shown as a function of energy for γ=2, assuming that the momentum dependence of the transition matrix elements does not vary with transition energy. As ω goes to zero, the $E1$ cross section approaches the semiclassical result. This is expected, as in this limit the argument of the logarithm is large in both the semiclassical expression and the high energy limit of the quantum calculation. As a result, the semiclassical piece of the quantum cross section dominates, and the two limits are the same. For large ω, both the $E1$ and $E2$ ratios are enhanced, and the degree of enhancement is quite sensitive to the behavior of the transition form factors. For small ω, the quantum $E2$ cross section is roughly four times the classical result, indicating that the large γ and small ω limits are not equivalent for higher multipoles.

In order to make a meaningful comparison with experiment, we must account for the final-state strong interactions between the target and projectile. The choice of $b_{\min}$ in Eq. (29) is designed to do exactly this for the semiclassical problem [11]. Briefly, $b_{\min}$ is chosen such that the mean number of nucleon-nucleon collisions, cal-

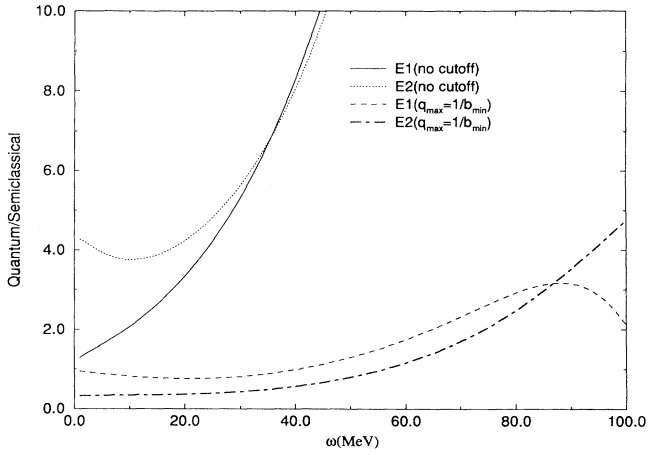

FIG. 5. Ratio of the quantum to classical excitation cross sections for ^{197}Au on ^{197}Au as a function of transition energy. The solid and dotted curves result from the full quantum mechanical calculation assuming no cutoff on the transverse momentum transfer, while the dashed and dot-dashed curves include a cutoff $q_{\max} = 1/b_{\min}$.

culated using the Glauber approach, at impact parameter $b = b_{\min}$ is exactly 1. For $b > b_{\min}$, the probability that a second nucleon will be knocked out of the target by the strong interaction drops rapidly to zero. For $b < b_{\min}$, the mean number of nucleon-nucleon collisions rises very rapidly, and the probability of at least one additional nucleon getting out of the target goes rapidly to 1. Hence, we obtain the usual semiclassical picture, where the equivalent photon number is calculated by integrating the field intensity from all trajectories with $b > b_{\min}$.

The same idea can be applied to the quantum picture by artificially including a maximum value, $q_{\max} \approx 1/b_{\min}$, for the transverse momentum transfer in the collision. The effect of this cutoff is to change the upper limit of the q integration in Eq. (28) to $\sqrt{q_0^2/\beta^2 + 1/b_{\min}^2}$ instead of ∞. In Figs. 2–5, the ratio of the new quantum and semiclassical cross sections is shown as a function of the projectile energy and transition frequency for the same projectile target combinations used previously. The same general trends hold; the quantum cross section is enhanced for small projectile energies, and approaches the semiclassical limit as γ gets large. (This latter fact holds because the cross section is dominated by the photon pole as $\gamma \to \infty$, so that the precise value of the high q cutoff becomes irrelevant.) Not unexpectedly, the size of the quantum cross section is smaller than in the case of no cutoff, with the result that the small γ enhancement of the cross section is less pronounced, and, for large γ, the semiclassical limit is approached from below, rather than above as before. Similar conclusions may be drawn regarding the transition frequency dependence of the cross section. As before, the small ω and large γ limits of the $E1$ cross section approach the classical result, while the two limits differ markedly for the quadrupole cross section. Perhaps the most noteworthy feature of the ω dependence is that the strong dependence of the cross section ratio on the transition form factors has been largely eliminated.

Of particular phenomenological interest is the 20–25 % suppression of the quantum $E1$ cross section relative to the semiclassical in the region $\gamma = 2$–3. This suppression is at precisely the right location and magnitude to explain the discrepancy between the WWF approximation and recent single neutron removal data for ^{238}U on ^{197}Au [12]. In Table I, we compare the results of our calculation and the WWF calculation with experimental data from Refs. [2,12]. For the heaviest projectiles, the agreement between the quantum theory and experiment is much improved over the WWF results. For Fe and Ar, the quantum theory does about as well as the semiclassical, and for the lightest two projectiles, the semiclassical theory does better.

TABLE I. Predictions of Weizäcker-Williams-Fermi and quantum theory for single neutron removal from ^{197}Au using the Goldhaber-Teller model for the transition densities. Data from Refs. [1,12].

		σ^{class} (mb)		σ^{quantum} (mb)		σ^{EXPT} (mb)
Proj	γ	$E1$	$E2$	$E1$	$E2$	
^{12}C	3.23	42	9	36	4	75±14
^{20}Ne	3.23	111	22	95	9	153±18
^{40}Ar	2.91	315	62	262	25	348±34
^{56}Fe	2.81	614	120	506	47	601±54
^{139}La	2.34	2190	462	1738	171	1970±130
^{238}U	2.0	4337	1045	3388	365	3160±230

This level of agreement with the quantum theory is in fact quite heartening. To begin with, the "experimental" numbers listed in Table I are not raw data, but rather the difference between the raw data and an estimate of the strong interaction contribution to the single neutron removal cross section. As noted in Ref. [11], estimates of the strong interaction contribution to the cross section are model dependent, so that an additional systematic uncertainty of at least 20 mb should be added to all the results listed in Table I. Clearly, for the heavy projectiles, this additional uncertainty is not important, as the extracted electromagnetic cross sections are quite large by comparison. For the lightest projectiles, however, the additional uncertainty is comparable to the extracted ED cross section, and is quite likely responsible for the observed discrepancies.

IV. CONCLUSIONS

Using a very simple model of nuclear structure, we have calculated the electromagnetic excitation cross section for nuclear collisions in first Born approximation, neglecting final-state interactions, and have found significant differences from results of the semiclassical WWF method. For $E1$ transitions, we find that the impact parameter cutoff required for the semiclassical calculation to agree with the high energy limit of the quantum cross section is significantly smaller than the phenomenological cutoffs used to analyze experiments. At energies less than a few GeV/nucleon, the cross section is enhanced over the semiclassical result by as much as 20% when the smaller cutoff is used. For $E2$ transitions, we find the cross section is significantly enhanced even at RHIC energies, and, unlike the $E1$ case, that the limit of small transition energy and large projectile energy are not the same.

When final-state interactions are included via a phenomenological cutoff, we find that the $E1$ cross section is greatly enhanced over the analogous WWF calculation for low projectile energies, while the cross section is suppressed at higher energies. The $E2$ cross section is suppressed by as much as factor of 3 for all but the lowest projectile energies. The low energy enhancement is relevant for electromagnetic dissociation studies of the low energy, pygmy resonances in neutron-rich nuclei such as ^{11}Li, and the suppression at higher energies resolves the conflict between single neutron removal experiments and the semiclassical theory for all but the lightest projectiles, where the data are very sensitive to systematic errors in the separation of the nuclear and electromagnetic contributions to the cross section.

While the agreement with data is extremely satisfactory given the simplicity of the Goldhaber-Teller model, a number of interesting questions remain. To begin, the

calculation should be redone using a realistic model for the projectile and target densities, including the widths of the giant resonance states, in order to improve the quantitative description of the data. This is particularly relevant for heavier targets, where the applicability of the Goldhaber-Teller model has been questioned [17]. In addition, the effect of additional photon exchanges should be studied, both to understand the effect of the repulsive Coulomb potential on the scattering process and to study the question of multiphonon excitations in the target nucleus. Finally, the process where both the target and projectile are excited, which should be non-negligible in target fragmentation experiments with light projectiles, should be calculated.

ACKNOWLEDGMENTS

The work of C.J.B. and J.L.F. was performed under the auspices of the U.S. Department of Energy. One of us (J.L.F.) would like to thank the Alexander von Humboldt-Stiftung for support.

APPENDIX A

In this appendix we sketch the cross section derivation for target excitation in a more familiar form, which highlights the nonrelativistic nature of the nuclear physics. It also allows us to point out our approximations (explicit or implicit) and to emphasize the role of gauge invariance, which puts the results into a form where Siegert's theorem can be applied immediately. We assume the following. 1. First Born approximation in the fine-structure constant α; this is required for tractability. 2. No target recoil, which presupposes that momentum transfers are very small compared to the target mass m_t; this greatly simplifies the kinematics. 3. The maximum momentum transfer can be replaced by infinity, for ease of performing integrations; in practice, small momentum transfers dominate. 4. A nonrelativistic description of the target nucleus, and of the *internal* structure of the projectile nucleus, is sufficient; the photonuclear response is almost entirely nonrelativistic, and most of what we know is based on this (successful) description. 5. Both target and projectile are spinless and only the former is excited; neither restriction is essential, but will simplify the derivation. 6. All purely hadronic contributions to the excitation amplitude can be ignored. Elastic Coulomb scattering is infinite and will also be ignored.

The current of the elastically scattered projectile is conserved and is given by $F_p(q^2)(P_f + P_i)^\mu/\sqrt{4E_fE_i}$, where the projectile charge distribution is present through its Fourier transform, the projectile form factor, $F_p(q^2)$. The latter is a function of the (squared) four-momentum transfer, $q^\mu = P_i - P_f$. The distinction between this quantity and the three-momentum transfer is a relativistic correction (and a recoil correction in the projectile rest frame). We consequently replace $F_p(q^2)$ by $F_p(\mathbf{q}^2) \equiv \int d^3x\, \rho_p(x)\, e^{i\mathbf{q}\cdot\mathbf{x}}$.

The target current is denoted by $\hat{J}^\mu(\mathbf{q}) = (\hat{\rho}(\mathbf{q}), \hat{\mathbf{J}}(\mathbf{q}))$ and is conserved. That is, $q_\mu \hat{J}^\mu(\mathbf{q}) \equiv 0$. Rewriting the kinematical factors in the projectile current, $(P_f + P_i)^\mu$, as $2P_i^\mu - q^\mu$, we can use current conservation and drop the q^μ factor. Thus, the current-current matrix element is given by $(E_i/E_f)^{\frac{1}{2}}\,[\rho_{N0}(\mathbf{q}) - \boldsymbol{\beta}\cdot\mathbf{J}_{N0}(\mathbf{q})]$, where $\boldsymbol{\beta} = \mathbf{P}_i/E_i$ is the projectile velocity and $J^\mu_{N0}(\mathbf{q}) \equiv \langle N|\hat{J}^\mu(\mathbf{q})|0\rangle$. The energy difference q_0 of the states labeled N and 0 is denoted by ω_N.

We wish to calculate the total cross section, which means that we must integrate over all of phase space. Ignoring recoil (which means that P_f^μ is independent of the scattering angle θ) we have for fixed energy transfer: $\mathbf{q}^2 = (\mathbf{P}_f - \mathbf{P}_i)^2 = P_f^2 + P_i^2 - 2P_fP_i\cos\theta$ or $d\mathbf{q}^2 = 2P_fP_i\sin\theta d\theta = d\Omega(2P_fP_i/2\pi)$, since the azimuthal dependence is trivial. All of the phase-space integrals (but one) can now be evaluated and we obtain

$$\sigma_{\rm WW} = \frac{4\pi Z_p^2\alpha^2}{\beta^2}\sum_{N\neq 0}\int_{\mathbf{q}^2_{\rm min}}^\infty \frac{d\mathbf{q}^2 F_p^2(\mathbf{q}^2)}{(\mathbf{q}^2-\omega_N^2)^2}|\rho_{N0}(\mathbf{q}) - \boldsymbol{\beta}\cdot\mathbf{J}_{N0}(\mathbf{q})|^2. \tag{A1}$$

This deceptively simple form has many aspects of complexity. The integral should be dominated by the pole in the photon propagator and the small values of $\mathbf{q}^2_{\rm min} = \omega_N^2/\beta^2$ and $q^2_{\rm min} = -\omega_N^2/\beta^2\gamma^2$. This further implies that electric dipole processes should dominate, because they are largest for small $\mathbf{q}^2$. This multipole should consequently not be very sensitive to F_p, unlike higher ones which are certain to be. In addition, we can make use of the conserved current to transform to Coulomb gauge. This eliminates the (redundant) longitudinal component of the current, and expresses the result in terms of transverse-current matrix elements (which determine photoabsorption) and purely Coulombic excitation. We also impose the no-recoil approximation in the form $P_i\cdot q/E_i = q_0 - \boldsymbol{\beta}\cdot\mathbf{q} = q^2/2E_i \sim 0$, so that we can replace $\boldsymbol{\beta}\cdot\mathbf{q}$ by $\omega_N(=q_0)$ where needed. We also impose current conservation: $\mathbf{q}\cdot\mathbf{J}_{N0}(\mathbf{q}) = \omega_N\,\rho_{N0}(\mathbf{q})$.

Expanding the squares of matrix elements and using the two spin-summed relationships

$$\sum_{\rm spins}\rho^*_{N0}(\mathbf{q})J^\alpha_{N0}(\mathbf{q}) = \frac{\mathbf{q}}{\mathbf{q}^2}\sum_{\rm spins}|\rho_{N0}(\mathbf{q})|^2\ , \tag{A2}$$

$$\sum_{\text{spins}} J^{\alpha}_{N0}(\mathbf{q}) J^{\beta *}_{N0}(\mathbf{q}) = \sum_{\text{spins}} \left[\frac{\omega_N^2}{\mathbf{q}^2} |\rho_{N0}(\mathbf{q})|^2 \delta^{\alpha\beta} + \left(|\mathbf{J}_{N0}(\mathbf{q})|^2 - \frac{3\omega_N^2}{\mathbf{q}} |\rho_{N0}(\mathbf{q})|^2 \right) \frac{(\delta^{\alpha\beta} - \hat{q}^{\alpha}\hat{q}^{\beta})}{2} \right] , \tag{A3}$$

leads to the (spin-summed) result

$$|\rho_{N0} - \boldsymbol{\beta} \cdot \mathbf{J}_{N0}|^2 = |\rho_{N0}(\mathbf{q})|^2 \frac{(\mathbf{q}^2 - \omega_N^2)^2}{\mathbf{q}^4} + \frac{1}{2} \left(\beta^2 - \frac{\omega_N^2}{\mathbf{q}^2} \right) \left[|\mathbf{J}_{N0}(\mathbf{q})|^2 - \frac{\omega_N^2}{\mathbf{q}^2} |\rho_{N0}(\mathbf{q})|^2 \right] . \tag{A4}$$

Note that the factor which multiplies (the first) $|\rho|^2$ cancels the photon propagator and substitutes the Coulomb one. Moreover, the quantity in square brackets is the *transverse* current (i.e., the full current minus the longitudinal part). This leads to the Coulomb gauge result

$$\sigma_{\text{WW}} = \frac{4\pi Z_p^2 \alpha^2}{\beta^2} \sum_{N \neq 0} \int_{\mathbf{q}^2_{\text{min}}}^{\infty} d\mathbf{q}^2 F_p^2(\mathbf{q}^2) \left\{ \frac{|\rho_{N0}(\mathbf{q})|^2}{\mathbf{q}^4} + \frac{\frac{1}{2}\left(\beta^2 - \frac{\omega_N^2}{\mathbf{q}^2}\right)}{(\mathbf{q}^2 - \omega_N^2)^2} \left[|\mathbf{J}_{N0}(\mathbf{q})|^2 - \frac{\omega_N^2}{\mathbf{q}^2} |\rho_{N0}(\mathbf{q})|^2 \right] \right\} . \tag{A5}$$

Using $\beta^2 = -\frac{1}{\gamma^2} + 1$ this can be rearranged into a form commensurate with Eq. (14), after we perform the $\mathbf{q}^2$ integrations. We use

$$J^{\mu}_{N0}(\mathbf{q}) = \int d^3x \, e^{i\mathbf{q}\cdot\mathbf{x}} \langle N | \hat{J}^{\mu}(\mathbf{x}) | 0 \rangle \tag{A6}$$

and the fact that there is no overall dependence on $\hat{q}$ after spin sums are performed, which leads to a slightly different form of Eq. (14):

$$\sigma_{\text{WW}} = \frac{4\pi Z_p^2 \alpha^2}{\beta^2} \sum_{N \neq 0} \frac{1}{\omega_N^2} \int d^3x \int d^3x' \Big\{ \rho_{N0}(\mathbf{x}) \rho^*_{N0}(\mathbf{x}') \left[\frac{I_2(y)}{\gamma^2} + I_3(y) \right] - [\mathbf{J}_{N0}(\mathbf{x}) \cdot \mathbf{J}^*_{N0}(\mathbf{x}') - \rho_{N0}(\mathbf{x}) \rho^*_{N0}(\mathbf{x}')] \left[\frac{I_1(y)}{\gamma^2} + I_2(y) \right] \Big\} . \tag{A7}$$

One projectile form factor has been folded into each charge and current matrix element. That is, $\rho_{N0}(\mathbf{x})$ is actually the convolution of a projectile (elastic) charge density with a target (transition) density. We have also used $y = \omega_N z = \omega_N |\mathbf{x} - \mathbf{x}'|$. This compact result in configuration space is finite, *requires* no cutoffs, and is relatively simple to work with.

The corresponding expression for the cross section for the absorption of a photon with energy, ω, can be developed in the same form:

$$\sigma_{\gamma}(\omega) = 2\pi^2 \alpha \sum_{N \neq 0} \frac{\delta(\omega - \omega_N)}{\omega_N} \int d^3x \int d^3x' \, j_0(y) \, [\mathbf{J}_{N0}(\mathbf{x}) \cdot \mathbf{J}^*_{N0}(\mathbf{x}') - \rho_{N0}(\mathbf{x}) \rho^*_{N0}(\mathbf{x}')] . \tag{A8}$$

Various sum rules can be constructed from this by integration:

$$\sigma_n \equiv \int d\omega \, \omega^n \sigma_{\gamma}(\omega) . \tag{A9}$$

In Appendix B the leading-order contributions are worked out in detail, including an analytic evaluation of the cutoff R_{ℓ} (for $\ell = 1$), in the context of a simple nuclear model.

APPENDIX B

Complete expressions including formulas for the cutoffs R_{ℓ} are difficult to develop. They will also differ from multipole to multipole. Nevertheless, because most of the photodisintegration cross section at low energies is unretarded electric dipole in nature, it is useful to investigate how the cutoff arises and estimate its size according to models of the electric-dipole transition density.

If one expands to lowest order in z [viz., $(z)^0$] the factors multiplying the current matrix elements $[\mathbf{J}_{N0}(\mathbf{x}) \cdot \mathbf{J}^*_{N0}(\mathbf{x}')]$ in Eq. (A7), only unretarded electric-dipole transitions can result. Using Siegert's theorem [15] to express the current in terms of the dipole operator, $\mathbf{D}$, and the excitation energy, ω_N,

$$\int d^3x \mathbf{J}_{N0}(\mathbf{x}) = i\omega_N \mathbf{D}_{N0} , \tag{B1}$$

one finds that the current terms contribute to the total disintegration cross section

$$\sigma_{\text{WW}} = \frac{4\pi Z_p^2 \alpha^2}{\beta^2} \sum_{N \neq 0} T_{N0} , \tag{B2}$$

an amount

$$T^{(J)}_{N0} = |\mathbf{D}_{N0}|^2 \left(\ln(\gamma) - \frac{\beta^2}{2} \right) . \tag{B3}$$

Note that these terms neither require nor generate a cutoff in the logarithm.

The corresponding constant factors multiplying $\rho_{N0}(\mathbf{x})\rho^*_{N0}(\mathbf{x}')$ give no net contribution to this order, since

$$\int d^3x\, \rho_{N0}(\mathbf{x}) = Q_{N0} \equiv 0 \ , \tag{B4}$$

because we have agreed not to include elastic scattering ($N \neq 0$). The first-order terms in z^2 generate elastic scattering plus electric-dipole transitions:

$$T^{(\rho)}_{N0} = \frac{1}{3}\int d^3x \int d^3x' \rho_{N0}(\mathbf{x})\rho^*_{N0}(\mathbf{x}')\, z^2 \ln(z) - \frac{2}{3}|\mathbf{D}_{N0}|^2\left[\ln\left(\frac{\omega_N}{\beta}\right) + \frac{1}{2}\ln(\gamma) + \gamma_E - \frac{11}{6} - \frac{\beta^2}{4}\right] , \tag{B5}$$

where γ_E is Euler's constant, $\mathbf{z} = \mathbf{x} - \mathbf{x}'$, and $z^2 = (x^2 + x'^2) - 2\mathbf{x}\cdot\mathbf{x}'$ has been used. Combining the charge and current contributions one obtains

$$T_{N0} = \frac{1}{3}\int d^3x \int d^3x' \rho_{N0}(\mathbf{x})\rho^*_{N0}(\mathbf{x}')\, z^2 \ln(z) + \frac{2}{3}|\mathbf{D}_{N0}|^2\left(\ln\left[\frac{\beta\gamma}{\omega_N}\right] - \gamma_E + \frac{11}{6} - \frac{\beta^2}{2}\right) . \tag{B6}$$

This can be rearranged into the conventional Weizäcker-Williams [7] form

$$T_{N0} = \frac{2}{3}|\mathbf{D}_{N0}|^2\left[\ln\left(\frac{2\beta\gamma}{\omega_N R_1}\right) - \gamma_E - \frac{\beta^2}{2}\right] , \tag{B7}$$

if we define

$$\ln(R_1/2) = -\frac{11}{6} - \frac{\int d^3x \int d^3x' \rho_{N0}(\mathbf{x})\rho^*_{N0}(\mathbf{x}')\, z^2 \ln(z)}{2|\mathbf{D}_{N0}|^2} . \tag{B8}$$

Given any (electric-dipole) transition density, the p-wave part of $z^2\ln(z)$ can easily be projected out and the double integral evaluated. The cutoff R_1 comes from the I_3 term in Eq. (A7), which itself comes solely from Coulomb scattering [i.e., the first term in Eq. (A5)].

If the integration variables in Eq. (B8) are changed to $\mathbf{z}$ and $\mathbf{x}'$, we find

$$\int d^3x \int d^3x' \rho_{N0}(\mathbf{x})\rho^*_{N0}(\mathbf{x}')\, z^2 \ln(z) = \int d^3z\, F_N(\mathbf{z})\, z^2 \ln(z) \ , \tag{B9}$$

where

$$F_N(\mathbf{z}) = \int d^3x'\, \rho_{N0}(\mathbf{z}+\mathbf{x}')\rho^*_{N0}(\mathbf{x}') \ , \tag{B10}$$

which is a convolution of transition densities. Elastic densities of this type have appeared in atomic calculations [18, 19]. This form is particularly convenient for deriving asymptotic forms, as well. The drawback is the required construction of the second-order (convoluted) transition density. We note that the logarithm in Eq. (B8) is the only one contained in $I_3(y)$, but it contributes to all Coulomb multipoles.

A complete model of the electric-dipole transition density is needed in order to construct $F_N(\mathbf{z})$. One such model is the Goldhaber-Teller model [16], which we sketch below. The transition charge operator $\rho_{N0}(\mathbf{x})$ can be represented by the surface-peaked function

$$\rho_{N0}(\mathbf{x}) \equiv \langle Nm|\hat{\rho}(\mathbf{x})|0\rangle = -\lambda_{N0}\, \hat{\boldsymbol{\epsilon}}^*_m \cdot \boldsymbol{\nabla}\rho_0(x) \ , \tag{B11}$$

where $\langle 0|\hat{\rho}(\mathbf{x})|0\rangle \equiv \rho_0(x)$ is the ground-state charge density, from which it follows that

$$\int d^3x\, \mathbf{x}\, \rho_{N0}(\mathbf{x}) = \lambda_{N0}\, \hat{\boldsymbol{\epsilon}}^*_m \equiv \mathbf{D}_{N0} \ . \tag{B12}$$

We have defined $\int d^3x\, \rho_0(x) = 1$ and used the spherical projection operators $\hat{\boldsymbol{\epsilon}}^*_m$ and the Wigner-Eckart [20] theorem to determine the dependence of the transition matrix element on the magnetic quantum number (m) of the final (dipole) state. For this model then, $|\mathbf{D}_{N0}|^2 = |\lambda_{N0}|^2$ and the last term in Eq. (B8) can be rewritten as

$$\int d^3x\, \rho_0(x) \int d^3x' \rho_0(x')[\ln(z) + \tfrac{5}{6}]$$
$$= \int d^3z\, \rho_{(2)}(z)[\ln(z) + \tfrac{5}{6}]$$
$$= \tfrac{1}{3} + \tfrac{1}{4}\int d^3x \rho_0(x) \int d^3x' \rho_0(x')\, [(x+x')^2 \ln(x+x') - (x-x')^2 \ln|x-x'|]/xx' \ , \tag{B13}$$

where the elastic counterpart of $F_N(\mathbf{z})$ is the Zemach density [18]:

$$\rho_{(2)}(z) = \int d^3x'\, \rho_0(|\mathbf{z}+\mathbf{x}'|)\rho_0(|\mathbf{x}'|) \ . \tag{B14}$$

The latter density plays a critical role in the nuclear-size modification of the hyperfine splitting [18] and Lamb shift [19] in atoms. Note that if ρ_0 is properly normalized, then $\rho_{(2)}$ is also. The final form in Eq. (B13) results from performing the average over the angle between $\hat{x}$ and $\hat{x}'$

contained in $\mathbf{z}$. This collective model then leads to the very simple result

$$\ln(R_1/2) = -1 + \int d^3z\, \rho_{(2)}(z)\, \ln(z)\ . \tag{B15}$$

To go further requires another model assumption. For simplicity we choose a uniform (liquid-drop) charge density: $\rho_0(r) = \frac{3\theta(R_t - r)}{4\pi R_t^3}$, which leads to

$$\rho_{(2)}(r) = \frac{3}{4\pi R_t^3}\,\theta(2R_t - r)\left(1 - \frac{3r}{4R_t} + \frac{r^3}{16R_t^3}\right)\ . \tag{B16}$$

The integral in Eq. (B15) has the value $\ln(2R_t) - \frac{3}{4}$, which leads finally to

$$\ln(R_1/2) = \ln(2R_t) - \tfrac{7}{4}\ , \tag{B17}$$

or $\frac{R_1}{R_t} = 0.695$, where $R_t = 1.2A_t^{\frac{1}{3}}$ fm.

This derivation ignores one important piece of physics. The projectile, as well as the target, has a finite size. Because in momentum space the form factors of initial and final projectile and target are all multiplied together, the projectile charge density will enter as a convolution with the (transition) density of the target. For example, folding the target density in the previous model (with radius R_t) with a projectile whose density is ρ_0' (with radius R_p) leads to a transition density

$$\begin{aligned}\hat{\rho}(\mathbf{x}) &= \int d^3x'\, \rho_0'(|\mathbf{x} - \mathbf{x}'|)\, \hat{\boldsymbol{\epsilon}}_m^* \cdot \boldsymbol{\nabla}' \rho_0(x') \\ &= \hat{\boldsymbol{\epsilon}}_m^* \cdot \boldsymbol{\nabla} \bar{\rho}_{(2)}(x)\ ,\end{aligned} \tag{B18}$$

where $\bar{\rho}_{(2)}$ is obtained by folding ρ_0 and ρ_0' together. Thus, we can use Eq. (B15) if we fold two densities ($\bar{\rho}_{(2)}$) together. This density, $\rho_{(4)}(x)$, can be shown to be independent of the order in which the folding is performed. Consequently, one can form $\rho_{(4)}$ by first folding two densities ρ_0 together, then separately folding together two densities ρ_0', and finally folding these two (folded) densities together.

The resulting forms are rather complicated, and we simply state the result

$$\begin{aligned}\langle \ln(z)\rangle = \int d^3z\, \rho_{(4)}(z)\, \ln(z) &= \ln\left(2(R_t + R_p)\right) \\ &+ (R_p - R_t)^8 \frac{(R_p + 2R_t)(R_t + 2R_p)(2R_p^2 + 11R_tR_p + 2R_t^2)}{2100 R_t^6 R_p^6} \ln\left|\frac{R_t - R_p}{R_t + R_p}\right| \\ &- R_p^4 \frac{(4R_p^2 - 81R_t^2)}{1050R_t^6} \ln\left(\frac{R_p}{R_t + R_p}\right) - R_t^4 \frac{(4R_t^2 - 81R_p^2)}{1050R_p^6} \ln\left(\frac{R_t}{R_t + R_p}\right) \\ &+ \frac{R_p^4}{525R_t^4} + \frac{R_t^4}{525R_p^4} + \frac{107R_t^2}{700R_p^2} + \frac{107R_p^2}{700R_t^2} - \frac{16661}{12600}\ .\end{aligned} \tag{B19}$$

There are two simple limits:

$$\lim_{R_p \to 0} \left[\langle \ln(z)\rangle - \ln\left(2(R_t + R_p)\right)\right] = -\tfrac{3}{4}$$

and

$$\begin{aligned}&\lim_{R_p \to R_t} \left[\langle \ln(z)\rangle - \ln\left(2(R_t + R_p)\right)\right] \\ &\quad = -\tfrac{11}{75}\ln(2) - \tfrac{1823}{1800}\ .\end{aligned} \tag{B20}$$

The terms in Eq. (B19) which supplement $\ln[2(R_t + R_p)]$ [which we denote by $s(\frac{R_p}{R_t})$] vary monotonically from -0.75 to -1.114 as R_p is varied from 0 to R_t. Thus we can rewrite Eq. (B15) as

$$\ln(R_1/2) = \ln[2(R_t + R_p)] - 1 + s\ , \tag{B21}$$

or

$$R_1 = \delta\,(R_t + R_p)\ , \tag{B22}$$

where $R_{p,t} = 1.2A_{p,t}^{\frac{1}{3}}$, and $\delta = 4e^{-1+s}$ varies from 0.70 to 0.48 for the range of variation of R_p above. Previously, a value of 1.0 was recommended [8].

Although the model used here can be criticized on the basis that it is too simple to be realistic, our derivation nevertheless represents an exact solution to the problem for a simple collective model of electric-dipole transitions (Goldhaber-Teller model with a uniform charge distribution) in the unretarded dipole limit. The troublesome cutoff is determined by details of the electric-dipole transition charge density.

Finally, we can express our results in a particularly simple and elegant form which emphasizes well-known photonuclear sum rules. We find

$$\sigma_{\mathrm{WW}} = \frac{2\alpha\,\sigma_{-1} Z_p^2}{\pi\beta^2}\left[\ln\left(\frac{2\beta\gamma}{\bar{\omega}R_1}\right) - \gamma_E - \frac{\beta^2}{2}\right]\ , \tag{B23}$$

where σ_{-1} is defined in Eq. (A9) and has the experimental value $0.22(2)A_t^{\frac{4}{3}}$ mb for medium to heavy nuclei, and $\bar{\omega}$ is the mean photon energy, which can be taken to be the giant resonance energy, $79A_t^{-\frac{1}{3}}$ MeV [21]. The factors in front of the bracket are (numerically) consistent with $Z_p^2 A_t^{\frac{4}{3}}/\beta^2\ \mu$b. The argument of the logarithm is $\xi\beta\gamma$, where ξ varies from 6.0 to 4.3 as R_p varies from 0 to R_t.

[1] J.C. Hill, F.K. Wohn, J.A. Winger, M. Khayat, M.T. Mercier, and A.R. Smith, Phys. Rev. C **39**, 524 (1989); M.T. Mercier, J.C. Hill, F.K. Wohn, and A.R. Smith, Phys. Rev. Lett. **52**, 898 (1984); M.T. Mercier, J.C. Hill, F.K. Wohn, C.M. McCullough, M.E. Nieland, J.A. Winger, C.B. Howard, S. Renwick, D.K. Matheis, and A.R. Smith, Phys. Rev. C **33**, 1655 (1986); J.C. Hill, F.K. Wohn, J.A. Winger, and A.R. Smith, Phys. Rev. Lett. **60**, 999 (1988); A.R. Smith, J.C. Hill, J.A. Winger, and P.J. Karol, Phys. Rev. C **38**, 210 (1988).

[2] M. Ishihara, Nucl. Phys. **A538**, 309 (1992).

[3] W.J. Llope and P. Braun-Munzinger, Phys. Rev. C **45**, 799 (1982).

[4] M.J. Rhoades-Brown and J. Weneser, Brookhaven Report No. BNL-47806, 1992 (unpublished).

[5] T.W. Donnelly and J.D. Walecka, Ann. Rev. Nucl. Sci. **25**, 329 (1975).

[6] V.M. Budnev, I.F. Ginzburg, G.V. Medelin, and V.G. Serbo, Phys. Rep. **15**, 181 (1975); D. Galetti, T. Kodama, and M.C. Nemes, Ann. Phys. (N.Y.) **177**, 229 (1988).

[7] E. Fermi, Z. Phys. **29**, 315 (1924); C.F. Weizäcker, *ibid.* **88**, 612 (1934); E.J. Williams, Phys. Rev. **45**, 729 (1934).

[8] C.A. Bertulani and G. Baur, Phys. Rep. **163**, 299 (1988), and references therein.

[9] J.D. Jackson, *Classical Electrodynamics* (Wiley, New York, 1975).

[10] At low energies, the equivalent photon flux varies significantly with multipolarity, and models are necessary to extract corrections to the naive Weizäcker-Williams-Fermi results. For a discussion of this, see W.J. Llope and P. Braun-Munzinger, Phys. Rev. C **41**, 2644 (1990); J.W. Norbury, *ibid.* **45**, 3024 (1992); C.J. Benesh, *ibid.* **46**, 2635 (1992).

[11] C.J. Benesh, B.C. Cook, and J.P. Vary, Phys. Rev. C **40**, 1198 (1989).

[12] D.D. Schwellenbach, J.C. Hill, F.K. Wohn, P.R. Graham, C.J. Benesh, A.R. Smith, D.L. Hurley, and P.J. Karol (unpublished).

[13] J.W. Norbury (unpublished).

[14] I.Y. Pomeranchuk and I.M. Shmushkevitch, Nucl. Phys. **23**, 452 (1961).

[15] J.L. Friar and S. Fallieros, Phys. Rev. C **29**, 1645 (1984).

[16] T. de Forest, Jr. and J.D. Walecka, Adv. Phys. **15**, 1 (1966).

[17] W.D. Myers, W.J. Swiatecki, T. Kodama, L.J. El-Jaick, and E.R. Hilf, Phys. Rev. C **15**, 2032 (1977).

[18] C. Zemach, Phys. Rev. **104**, 1771 (1956).

[19] J.L. Friar, Ann. Phys. (N.Y.) **122**, 151 (1979).

[20] A.R. Edmonds, *Angular Momentum in Quantum Mechanics* (Princeton University, Princeton, 1960).

[21] O. Bohigas, in *From Collective States to Quarks in Nuclei*, Proceedings of the Workshop on Nuclear Physics with Real and Virtual Photons, Bologna, Italy, 1980, edited by H. Arenhövel and A.M. Sarius, Lecture Notes in Physics Vol. 137 (Springer, Berlin, 1981), p. 65.